

FRACTALS FOR MODELLING AND ANALYSING GEO-INFORMATION

Mihai Datcu^{*}, Klaus Seidel
ETH Zurich

Institut für Kommunikationstechnik
Fachgruppe Bildwissenschaft
Gloriastr. 35, CH-8092, Zurich
tel:4112565352, fax:4112613429

^{*}on leave from:

Facultatea de Electronica si Tc.&CTS
Institutul Politehnic Bucuresti, Romania

1. Introduction

The high complexity of the remotely sensed images and measurements provided by the last generations of sensors demand new techniques for scene understanding and analysis. The similarity of fractal and real world objects was observed and intensively studied from the very beginning. The fractal geometry became a tool for computer graphics and data visualisation in the simulation of the real world. In order to perform visual analysis and comparisons between natural and synthetic scenes several techniques have been developed. After a period of qualitative experiments fractal geometry began to be used for objective and accurate purposes: modelling image formation processes, generation of geometrically and radiometrically accurate synthetic scenes and images, evaluation of the characteristics of the relief, determination of the surface roughness, analysis of textures. The techniques based on fractals show promising results in the field of image understanding and visualisation of high complexity data.

In the aim to give an introduction to the theory of fractals the following topics will be summarised in this paper: the definition and analysis of fractals based on self-similarity and self-affinity behaviours, definitions for fractal dimension, fractal synthesis, the projection properties of fractal surfaces. The derived techniques with applications in geo-information processing and understanding will be underlined: synthetic DEMs generation, fractal resampling of actual DEMs, algorithms for computation of the fractal dimension, multiresolution analysis of fractal images, multiresolution analysis and fractal dimension estimation.

The paper presents also several experiments done by the authors using fractals to generate accurate models for landforms and cover types, synthetic images generation for model based picture processing, and image processing techniques for remotely sensed images analysis and sensor fusion.

2. Elements of fractal geometry

A discussion of the field of fractals obviously embraces an enormous field (Peitgen, 1992). The primary concern of this chapter is thus with the presentation of the elementary ideas necessary to understand applications of fractal geometry in geo-information processing (Turcotte, 1992).

Fractal geometry deals with the behaviours of sets of points S , in the n -dimensional space R^n .

$$S \subset R^n \quad (1)$$

For the addressed applications S is a curve, a surface or an image intensity field. That why n will be restricted to 1, 2 or 3. But several applications, as multispectral data analysis, ask for representation of data in higher dimension space (Dodd, 1987).

2.1 Self-similarity and self-affinity

Mandelbrot defined a fractal as a shape made of parts similar to the whole in some way (Mandelbrot, 1982). The definition is qualitative but not ambiguous, as looks at the first glance. The main behaviour of a fractal is its self-similarity (Hata, 1989). A set is said **self-similar** if it can be expressed as a union of sets, each of which is a reduced copy of the full set. More general a set is said **self-affine** if it can be decomposed into subsets that can be linearly mapped into the full set. If the linear mapping is rotation, translation or isotropic dilatation the set is self-similar. The self-similar objects are particular cases of self-affine ones.

$$\{SELF - AFFINE\} \supset \{SELF - SIMILAR\} \quad (2)$$

A fractal object is self-similar or self-affine at any scale. If the similarity is not described by deterministic laws stochastic resemblance criteria can be found. Such an object is said to be **statistical self-similar**. The natural fractal objects are statistical self-similar. A statistical self-similar fractal is by definition isotropic.

To have a more precise, quantitative, description of the fractal behaviour of a set, a measure and a dimension are introduced (Baldo, 1990). The rigorous mathematical description is done by the Hausdorff's measure and dimension (Belair, 1989; Falconer, 1992).

2.2 Hausdorff dimension

Let \mathbf{S} be a set of points in the \mathbf{n} dimensional space $\mathbf{R}^{\mathbf{n}}$. The topological dimension of the space is \mathbf{n} , \mathbf{n} is an integer. Choose also a real number \mathbf{r} inferior to \mathbf{n} [3].

$$S \subset \mathbf{R}^{\mathbf{n}}; 0 \leq r \leq n \quad (3)$$

One consider further the cover $\mathbf{H}_{\delta}^{\mathbf{r}}$ of the set \mathbf{S} with sets \mathbf{U}_i of limited diameter $|\mathbf{U}_i|$ [5].

$$\mathbf{H}_{\delta}^{\mathbf{r}}(\mathbf{S}) = \inf \left\{ \sum_i |\mathbf{U}_i|^{\mathbf{r}} / 0 < |\mathbf{U}_i| < \delta \right\} \quad (4) \quad |\mathbf{U}| = \sup \{ |x - y| / x, y \in \mathbf{U} \} \quad (5)$$

The infimum is evaluated over all coverings of \mathbf{S} by a collection of sets with diameters at most δ . The set $\{\mathbf{U}_i\}$ is countable or finite. $\mathbf{H}_{\delta}^{\mathbf{r}}$ increases as δ decreases to zero. Decreasing δ the restrictions on the allowable coverings of the set \mathbf{S} are increasing.

The r -dimensional Hausdorff measure $\mathbf{H}^{\mathbf{r}}(\mathbf{S})$ of the set \mathbf{S} is defined:

$$\mathbf{H}^{\mathbf{r}}(\mathbf{S}) = \lim_{\delta \rightarrow 0} \mathbf{H}_{\delta}^{\mathbf{r}}(\mathbf{S}) \quad (6)$$

To exemplify: if \mathbf{S} is a smooth curve, \mathbf{U}_i can be a linear stick of length δ and $\mathbf{H}^1(\mathbf{S})$ is the length of the curve, if \mathbf{S} is a smooth surface, \mathbf{U}_i can be a disk of diameter δ and $\mathbf{H}^2(\mathbf{S})$ is the area of the surface. The Hausdorff measure generalizes the definition of length, area, volume. $\mathbf{H}_{\delta}^{\mathbf{r}}(\mathbf{S})$ gives the volume of e set \mathbf{S} as measured with a ruler of δ units. A figure with finite length will have zero area, and a finite area will be covered by a curve of infinite length.

Based on these observations and particular cases, two properties of the Hausdorff measure will be introduced. If the \mathbf{r} -dimensional Hausdorff dimension of the set \mathbf{S} is higher than zero, than the \mathbf{p} -dimensional Hausdorff measure of the set \mathbf{S} is infinite, for \mathbf{p} less than \mathbf{r} . If the \mathbf{r} -dimensional Hausdorff measure of the set \mathbf{S} is bounded, than the \mathbf{p} -dimensional Hausdorff measure of the set \mathbf{S} is zero, for \mathbf{p} greater than \mathbf{r} [5].

The value of the parameter \mathbf{r} for which the \mathbf{r} -dimensional Hausdorff measure of the set jumps from zero to infinite is said the *Hausdorff dimension*, $\mathbf{dim}_{\mathbf{H}}$, of the set \mathbf{S} [8].

$$\mathbf{H}^{\mathbf{r}}(\mathbf{S}) > 0; \forall p < r; \mathbf{H}^{\mathbf{p}}(\mathbf{S}) = \infty \quad (7)$$

$$\mathbf{H}^{\mathbf{r}}(\mathbf{S}) < \infty; \forall p > r; \mathbf{H}^{\mathbf{p}}(\mathbf{S}) = 0$$

$$\mathbf{dim}_{\mathbf{H}} \mathbf{S} = \sup \{ r / \mathbf{H}^{\mathbf{r}}(\mathbf{S}) = \infty \} \quad (8)$$

$$\mathbf{dim}_{\mathbf{H}} \mathbf{S} = \inf \{ r / \mathbf{H}^{\mathbf{r}}(\mathbf{S}) = 0 \}$$

A set is said fractal if its Housdorff dimension strictly exceeds its topological dimension.

$$\dim_{\mathbf{H}} S > n \quad (9)$$

Numerical evaluation of Hausdorff dimension is difficult because of the necessity to evaluate the infimum of the measure over *all* the coverings of the set of interest. That is the reason to look for other definition for the dimension of a set.

2.3 Minkowski dimension

Minkowski dimension (Baldo, 1990) allows the evaluation of the fractal feature of a set. First the parallel set $E_S(\delta)$ of the set S is introduced [8].

$$E_S(\delta) = \{x \in \mathbf{R}^n / d(x, S) \leq \delta\} \quad (10)$$

The parallel set $E_S(\delta)$ of the set S is the set including all the points of the space that are closer than a given constant δ to the points of the set S . The Minkowski dimension of the set S , is:

$$\kappa(S) = \lim_{\delta \rightarrow 0} \sup \left\{ n - \frac{\log V_n(E_S(\delta))}{\log(\delta)} \right\} \quad (11)$$

V_n represents the volume in the n dimensional space \mathbf{R}^n .

In contrast to the box counting dimension or the Hausdorff dimension, to compute Minkowski dimension one must not search for an optimal cover of the set S .

In figure1 is exemplified the parallel set (the Minkowski sausage) of a fractal curve. Computing the volume of the parallel sets for different values of the radius d , and plotting these values in log-log coordinates, one will obtain a straight line if the set has fractal behaviour. The Minkowski dimension is computed as the topological dimension of the space, n minus the slope of the straight line. The similarities in the structure of the set S are detected evaluating the volume of the associated parallel set for different scales defined by δ .

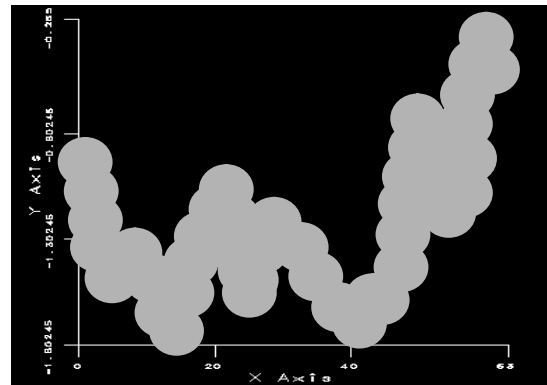


Fig. 1 Minkowski sausage

2.4 Box counting dimension

The box counting dimension allows evaluation of the dimension of sets of points spread in an n -dimension space and also gives possibilities for easy algorithmic implementation.

Given a set of points S , in a n -dimensional space \mathbf{R}^n , and N_δ is the least number of sets of diameter at most δ that cover S , the box counting dimension, $\dim_{\mathbf{B}}$, is defined as:

$$\dim_{\mathbf{B}} S = \lim_{\delta \rightarrow 0} \frac{\log N_\delta(S)}{-\log(\delta)} \quad (12)$$

Depending on the geometry of the box and the modality to cover the set, several box counting dimension can be defined: 1) the least number of closed balls of radius δ that cover S , 2) the least number of sets of diameter at most δ that cover S , 3) the least numbers of cubes of side δ that cover S , 4) the number of cubes of the lattice of side δ that intersect S , 5) the largest number of disjoint balls of radius δ centred in S (Falconer, 1990).

The equivalence of these definitions was proved. Also it was proved that these dimensions are

inferior bounded by the Hausdorff dimension (Dubuc, 1990).

In figure 2 the fourth definition is exemplified. A rectangular mesh of constant δ is overlapped on the erratic line. The 26 “cubes” of the lattice that intersect the set are marked in black. Using the box counting dimension, for the evaluation of the properties of discrete data sets, as always happens in real cases, careful interpretation of the results is asked. Different definitions give dimension with different properties and can have different values for the same set.

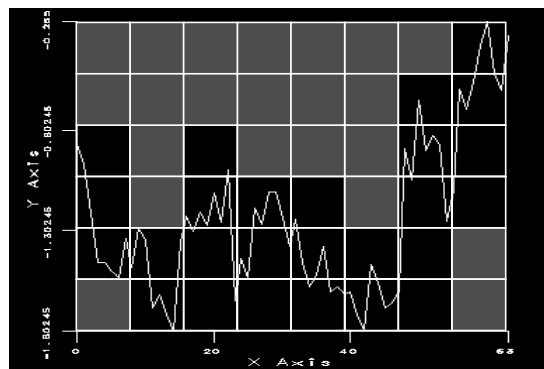


Fig. 2 Box counting dimension

To relate the scale properties of a fractal to the box counting dimension's definition follows an example. Consider a fractal self-similar contour $\mathbf{f}(\mathbf{x},\mathbf{y})$, $\mathbf{f}(\alpha\mathbf{x},\alpha\mathbf{y})$ is statistically similar to $\mathbf{f}(\mathbf{x},\mathbf{y})$; α is the scaling factor. The number of boxes of dimension δ_x, δ_y necessary to cover the set represented by the points of $\mathbf{f}(\mathbf{x},\mathbf{y})$ is \mathbf{N} , and the number of boxes of dimension $\alpha\delta_x, \alpha\delta_y$ required to cover the set is \mathbf{N}_α . If the set is self-similar, as previously supposed, the ratio $\mathbf{N}_\alpha/\mathbf{N}$ will be a constant. The logarithm of this constant is proportional with the fractal dimension of the set.

If a statistical self-affine fractal is considered it will be non-isotropic. At different scales $\mathbf{f}(\mathbf{x},\mathbf{y})$ will be statistically similar to $\mathbf{f}(\alpha\mathbf{x}, \alpha^{\mathbf{H}}\mathbf{y})$. \mathbf{H} is the Hausdorff dimension, and α is the scaling factor. The boxes must be scaled differently in x and y direction, with α and respectively $\alpha^{\mathbf{H}}$. The ratio $\mathbf{N}_\alpha/\mathbf{N}$ is also a constant proportional to fractal dimension of the set.

2.5 Other dimensions

Several others definitions for the dimension of a set have been introduced. All these definitions, as the previous ones also, have a common goal: to make evidence of the self-similarity or self-affinity of the set. As an immediate consequence all definition are based on a multiscale evaluation of a certain measure. For example:

P(m,L) dimension (Voss, 1986), is the probability to have \mathbf{m} points within a box of size \mathbf{L} . The expected number of boxes to cover the set $\mathbf{N}(\mathbf{L})$ is:

$$N(L) = \sum_{m=1}^N \frac{1}{m} P(m, L) \quad (13)$$

and the regression of \mathbf{N} versus \mathbf{L} in log-log plot gives a straight line if the set is a fractal one. The slope of the line is the fractal dimension of the given set.

Space scale filtering, the self-similarity or self-affinity properties of sets are scale relative, that is why one can deal with the change of the scale of the set instead of the change of magnitude of the “stick” he uses for the estimation of the dimension. For evaluation of the fractal dimension of a signal, ϕ , a multiresolution approach is used (Mussigmann,1990). The signal is smoothed using a bank of Gaussian filters having different variance, σ [14].

$$\Phi(\bar{x}, \sigma) = \int_{-\infty}^{\infty} \varphi(\bar{\xi}) \frac{1}{\sigma\sqrt{2\pi}} e^{-\frac{(\bar{x}-\bar{\xi})^2}{2\sigma^2}} d\bar{\xi} \quad (14)$$

The regression of the “length” of the signal, Φ measured with a fixed stick, plotted in log-log as a function of the variance of the applied filter will be a line. The slope of the line gives the fractal dimension.

Covering-blanket method, is used for the estimation of the fractal dimension of contours, surfaces or image intensities (Peli, 1900). The concept of covering-blanket is based on the analysis of a multiscale construction. For

a surface, as an example, the upper, and lower bounding surfaces are to be generated. The covering-blanket is defined by the band of thickness 2ϵ , created by the two secondary functions. The multiscale analysis will be done for different values of ϵ .

The estimation of the fractal dimension involves taking the logarithm of the difference of the upper and lower bounding surfaces divided by the scale factor ϵ , and fitting a line to it in a log-log plot, as function of scale.

Power-spectrum method, is based on the property of fractal functions to have a negative power-law shaped power-spectrum function (Voss, 1985). The Fourier transform is used to derive the power-spectrum and, a linear regression is used in log space to derive the fractal dimension.

Wavelet transform of fractals. Both fractals and wavelets, as main characteristic, allow the scale to be made explicit (Freeland, 1990). The wavelet transform Wf of a function $f(x)$ is its decomposition on a orthogonal basis of function. The basis of functions is generated from a parent function ψ using dilatations of factor a , and translations with vector b (Mallat, 1989).

$$Wf(a, b) = \int_{-\infty}^{\infty} f(x) \sqrt{a} \Psi(a(x-b)) dx \quad (15)$$

The wavelet transforms encodes patterns occurring at different scales in a uniform way. It means that considering a fractal and computing its wavelet transform one can derive the fractal dimension (Wornell, 1990).

3 Fractals synthesis

Brownian process. To generate fractal objects several techniques have been developed: deterministic fractals are synthesised using iterative equations, cellular automata, or L-systems; stochastic fractals are obtained by Brownian process simulation, using 1/f filtering methods, random_midpoint displacement or modified L-systems. Natural landforms are well represented by fractals derived from the Brownian process description (Voss, 1988).

Consider, in one dimension case, a random process $X(t)$. If the Probability Density Function PDF, of the consecutive samples is Gaussian the process is said **Brownian**.

$$\begin{aligned} X(t_{n+1}) - X(t_n) &= x(t_n) & t_{n+1} - t_n &= t \\ p(x, t) &= \frac{1}{\sqrt{4\pi St}} \exp\left(-\frac{x^2}{4St}\right) \end{aligned} \quad (16)$$

The Brownian motion describes as Gaussian the displacement of a particle in one time interval (Feder, 1989). The displacement is a independent variable. S is a constant: the diffusion coefficient, it models the “spread” of a particle trajectory in Brownian motion. To study the scale behaviours, the Brownian process will be sampled at intervals $\Theta = kt$. The PDF of the consecutive samples difference, for the new process, will be derived.

$$\Theta = kt; \zeta = t\sqrt{k} \quad p(\zeta, \Theta) = \frac{1}{\sqrt{k}} p(x, t) \quad (17)$$

The newly derived PDF at the scale $\Theta = kt$ is also Gaussian and differ by a constant from the original process PDF. The Brownian process is statistically self-affine. The affinity is in the statistic of the differences of consecutive samples at any scale. Wiener introduced a random function to describe the displacement of particle in Brownian motion. The difference of consecutive samples is extracted from a Gaussian distribution and is proportional with a power function of the sampling period (Mandelbrot, 1982).

$$X(t_{n+1}) - X(t_n) \approx grv |t_{n+1} - t_n|^H \quad (18)$$

Where grv is a Gaussian Random Variable, and $H = 1/2$. The process is self-affine.

Mandelbrot generalized the random function of Wiener and introduced the concept of fractional Brownian motion, changing the exponent H to be any real number in the interval $(0,1)$. The new random function was denominated $B_H(t)$. The previously presented random functions give a base for the generation of fractals in one dimension or in a n -dimensional space. The random functions can be represented in n -dimensions simply by the substitution of time in a space n -tuple of coordinates (Petland, 1984). Voss introduced the successive random addition algorithm (Voss, 1988). In order to generate a fractional Brownian curve the variance of the increments of the position must be:

$$V(t) = E \{ [X(t) - X(0)]^2 \} = |t|^{2H} \sigma_0^2 \quad (19)$$

In the first iteration the increments of the process are to be extracted from a Gaussian distribution of variance $\sigma = 1$. In the n -th iteration the displacements (midpoints) are interlaced between the previous step points, and are extracted from a Gaussian distribution of variance:

$$\sigma_n^2 = \left(\frac{1}{2}\right)^{2H} \sigma_{n-1}^2 \quad (20)$$

Spectral method The power spectral density S , of a self-affine fractal is a negative power law shaped function (Mandelbrot, 1986).

$$S(f) \approx 1/f^\beta \quad (21)$$

The fractal dimension D is related to the β coefficient (Voss, 1986):

$$D = T + (3 - \beta) / 2 \quad (22)$$

T is the topological dimension. As a direct consequence of this property the Fourier transform is one of the main tools for the generation of fractals objects.

L-systems. The plants three dimensional structure is probably the most realistic modelled using L-systems (Prusienkiewicz, 1989). A formal set of rules specify how the plants do develop themselves in different stages. It is important to develop algorithms which by means of a reduced set of parameters can control the variability of the synthetic vegetation. The L-system is constructed starting with a string called axiom, and in the first step substitute every symbol of the string in accordance to a given set of rules. The process is repeated iteratively. It is essential to note that all the symbols in the string are changed simultaneously. This is a major difference compared with a formal language where the parser is applied sequentially. Applying the previous procedure the defined object grows preserving the same structure at larger scales. More general than plant modelling, the L-systems can describe almost any fractal object or at least their finite approximations. The simplest class of L-system, DOL-system is exemplified further:

$$\begin{array}{l} \text{rule} \quad \mathbf{a} \rightarrow \mathbf{ab} \quad \mathbf{b} \rightarrow \mathbf{a} \\ \text{evolution} \quad \mathbf{b} \quad \mathbf{a} \quad \mathbf{ab} \quad \mathbf{aba} \quad \mathbf{abaab} \quad \mathbf{abaababa} \end{array} \quad (23)$$

The work of Lindenmayer was oriented mainly to graphic representation and considering the evolution of the field this issue was continued. The theory of L-systems developed in several new techniques: bracketed L-systems, a graph theoretic trees using strings with brackets (Lindenmayer, 1968); data base amplification (Smith, 1984), simulation of development of real plants; axial tree (Preparata, 1973), notion which complements the graph-theoretical concept and makes it closer to natural vegetation models; context-sensitive L-systems, that models the possible interaction of component elements. The techniques for plant models generation was enhanced using combined methodology of L-systems and iterated function systems IFS (Smith, 1991).

4 Applications of fractal geometry in geo-information processing

4.1 Synthesis

Synthetic Digital Elevation Models. Many of the very beginning applications of the fractal geometry were involved in finding methods for the generation of pleasant visual aspect images for computer graphic representations (Fournier, 1982). More recently realistic looking landscapes have been synthesised for flight simulators or other planets relief visualisation (Peitgen, 1992), and more, precise simulations of the landforms are derived in the aim to build models to be used in features evaluation for further correlation with natural relief 's characteristics (Clarke, 1988). Geomorphology and soil science ask for terrain models with peculiar characteristic for other simulations: water erosion process, drainage basins topology, surface water flow, river's course erosion, wind mass transport effects, deforestations, volcanic lava flow (Goodchild, 1982; Datcu, 1992). One of the cartography benefit from fractal simulation is the possibility to generate synthetic digital elevation models (DEM) at a variety of scales and terrain roughness which to be used as test areas for the performance of the algorithms for digitizing the simulated cartographic maps (Yokoya, 1989).

The techniques frequently used for the generation of synthetic DEMs are the "mid point displacement", previously presented, and the simulation of the $1/f$ noise.

A Gaussian white noise is filtered using a $1/f^\beta$ shaped transfer function. The output signal is a self-affine fractal having the fractal dimension $D = T + (3 - \beta)/2$. T is the topologic dimension of the space (Peitgen, 1988). The algorithm is presented in figure 3 (See ch..3, eq.21). Figure 4 shows two synthetic DEMs having different fractal dimension. The surfaces are presented as Lambertian surfaces illuminated from the S-E direction. The left side image, due to the fractals behaviour, can be any rescaled subwindow from the right side image. The surface is self-affine, in statistical sense. The "lakes" in the right side image are obtained as the intersection of a plane with the surface. The contours of the lakes are fractal lines having the fractal dimension $D - 1$ (Petland, 1984).

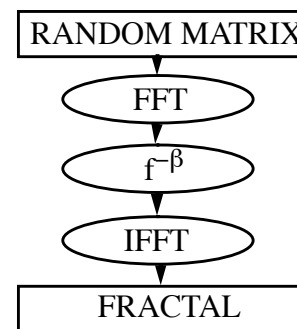


Fig.3 Algorithm for fractal DEM synthesis

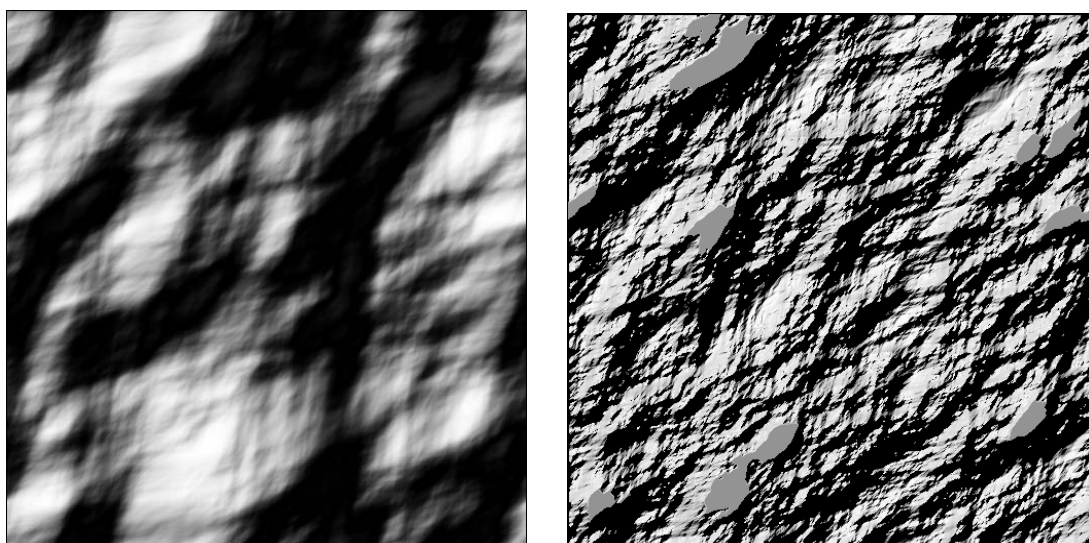


Fig.4 Synthetic fractal DEM presented as Lambertian surface illuminated from S-E.

Fractal resampling of real DEMs

The available DEMs are generally limited in resolution. The resolution is given by the constant of the support grid for the height data. Applications as: relief visualisation, image formation modelling for remote sensors, high resolution contour map elaboration, ask accurate DEMs. A higher resolution can be obtained by a resampling process: to add new samples in a higher resolution grid. If functional resampling is used the resulting DEM has an unrealistic smooth aspect. It was experimentally proved that the natural relief has fractal behaviour

for a certain range of scales (Goodchild, 1980;Turcotte,1992). The fractal resampling process uses this prior information: the similarity of landforms for several spatial scales. The fractal resampling method has two parts: the analysis of the real DEM for evaluation of the fractal dimension and local variance of the height field, and the fractal interpolation (Polidori, 1990; Yakoya, 1989).The method is depicted in figure 5 (See ch.3 eq.19). The fractal interpolation increases the resolution of the DEM in steps x2 (figure 6). The statistical resemblance of the synthesised samples is obtained using the random addition method of Voss (see ch.3). An example is presented in figure 7: an 100 m resolution DEM resampled to 50 m. The surface is presented as a Lambertian one, lighted from S-E. The visual appearance is more realistic but not only, other applications where the exactitude of the DEM is required in stochastic sense are of practical importance. The generation of synthetical images in the aim to enhance the performance of classification for remotely sensed images is one of the topics of interest (Seidel, 1993). The fractal resampling can not be applied down a given scale. Gravity and diffusion process or, vegetation cover broke the continuity in similarity, and other models must be applied (Clarke, 1991). At last it can be considered that fractal resampling is a computer graphic technique for surface representation applied in geo-science.

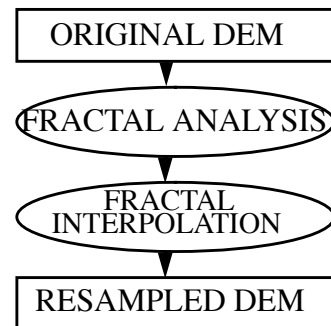


Fig.5 The algorithm for fractal resampling of DEM

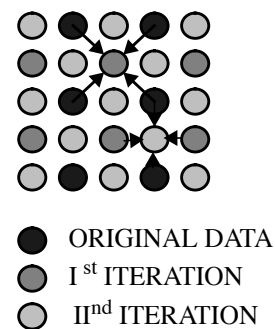


Fig.6 Fractal interpolation

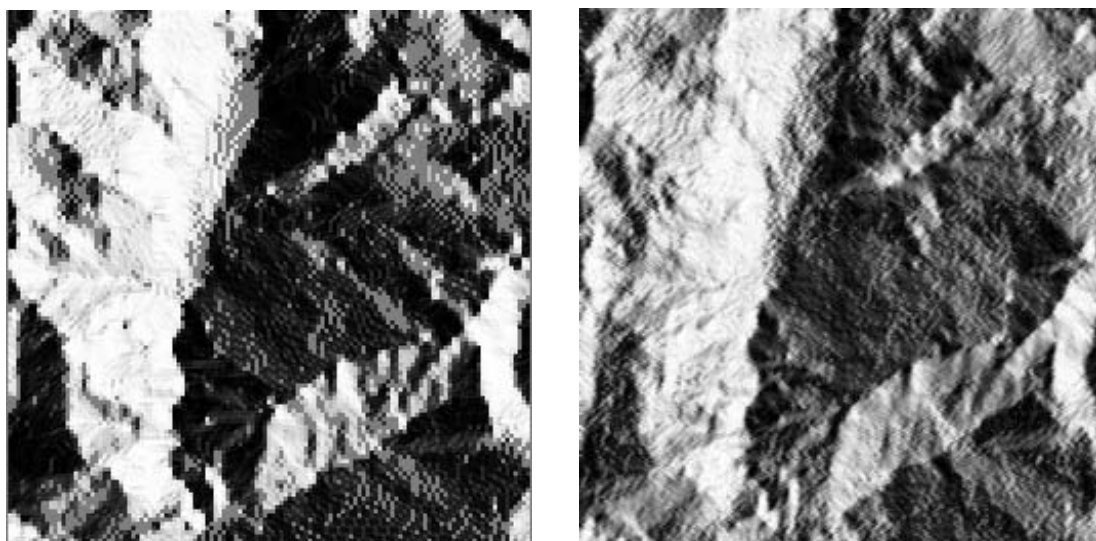


Fig.7 DEM: 100m resolution, fractal resampled DEM: 50m resolution

Virtual radiometric experiment

The prior knowledge of the radiometric signature of the land surface and cover is of recognized importance in photogrammetry and in model based recognition of the remotely sensed images. Accurate image synthesis or image formation simulation is possible only if the imaging system is well understood. It means the knowledge of the sensor, lighting system, and light interaction with the imaged surface. Existing computing graphics techniques make available the basic surface appearance models: diffuse, specular, Phong, multiple reflections (Glassner, 1991). The 3-D representation of surfaces is done by triangulation. Each microfacet has a surface appearance attribute. If the sensor resolution is lower than the resolution of the surface, the intensity of one pixel is modelled by the integral of all scattered intensities of the microfacets weighted by the sensor's spread point function. The virtual radiometric experiment can be done for a given sensor and micro-geometry of the surface. In figure 8 is presented the imaging geometry for a rough surface. Each microfacet is characterised by the surface optical attributes and its geometry, the local normal vector \bar{n} . The sensor and source of light positions are specified respectively by the vectors \bar{v} and \bar{l} . An area of 32 x 32 microfacets was imaged from a nadir placed sensor with variable incident illumination. The resulting images are displayed in figure 9. The last scene is a perspective view of the imaged surface (3D). Using the information from these images the albedo and BRDF can be computed, and with prior knowledge of the sensor characteristics the accurate pixels intensities can be modelled. The experiment explains the difference in radiometry of the images in figure 8. After a fractal resampling the local roughness increases and the BRDF is modified. The experiment was applied for vegetation cover radiometric evaluation (Goel, 1990). A three dimensional plant model was developed using generalised L-systems.

To take into account the exact surface roughness and to calculate the actual scattering cross-section the Kirchoff solution must be found. The validity of Kirchoff solution was intensively studied (Soto-Crespo, 1989). In the solution of scattering from fractal surfaces, the wavelength is considered as yardstick. The solution is derived for relative space-scale to wavelength ratios (Jaggard, 1990). The results find applicability to synthetic aperture radar (SAR) imagery of sea surface or rough terrain.

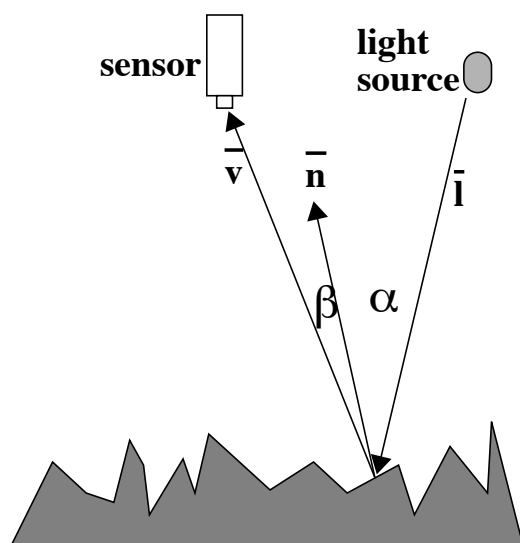


Fig.8 Imaging geometry

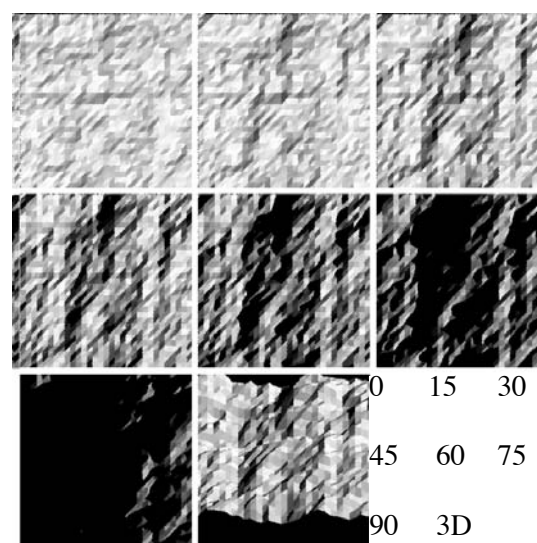


Fig.9 Rough surface imaged for different incident light position; 0, 15, 30, 45, 60, 75, 90 degrees

4.2 Analysis

The rough structure of many natural surfaces is reflected in a corresponding roughness of the pixel intensity of the imaged scene. The image is textured. If the surface is a fractal one, its image (the set of pixel intensities) will be also a fractal having the same dimension (Petland, 1984). The idea is to use fractal geometry, the fractal dimension, as a feature to characterise the textures. A fractal transform is defined: an image is mapped in an other image that have as pixel intensity the values of the fractal dimension derived for a moving window overlapped on the original picture. It is necessary to state here several observations: one can derive a large class of very different objects having the same fractal dimension, real structures have fractal behaviours for several ranges of the scale, could be possible that the similarity is respected only for a very low number of scales, the natural scenes when imaged are very often corrupted by strong noise, the sampling and quantification process destroy the scale invariant patterns. Several algorithms have been derived to enhance the discriminatory power of the fractal transform: multiple resolution techniques (Peleg, 1984), lacunarity (Mandelbrot, 1983; Keller, 1989), local fractal dimension (Mussingann, 1992), dendronic analysis (Hanusse, 1992). The rough aspect of the Synthetic Aperture Radar (SAR) images rises difficult problems in scene segmentation. The presence of the speckle phenomenon affects the performance of the algorithms for texture classification. In the mean time the filters applied to reduce the speckle noise change the texture features. The fractal dimension seems to be a promising global parameter for the classifications of the SAR images (Dellapiane, 1991; Allinson, 1990; Schistadt, 1992). In figure 10, a SAR (ERS-1) image and its fractal transform are presented. The fractal transform was locally evaluated using the $P(m,L)$ definition of the dimension (See ch. 2.5). The urban area is segmented. Taking into account the previous observations referring to the difficulties to interpret the values of the various dimensions, the fractal transform is generally used as a feature in fusion with other parameters. Much better results in the applications of the fractal transform are reported in the segmentation of the images obtained from optical sensors and in the classification of the terrain roughness and geological features (Polidori, 1991; Huang, 1990, Turcotte, 1992).

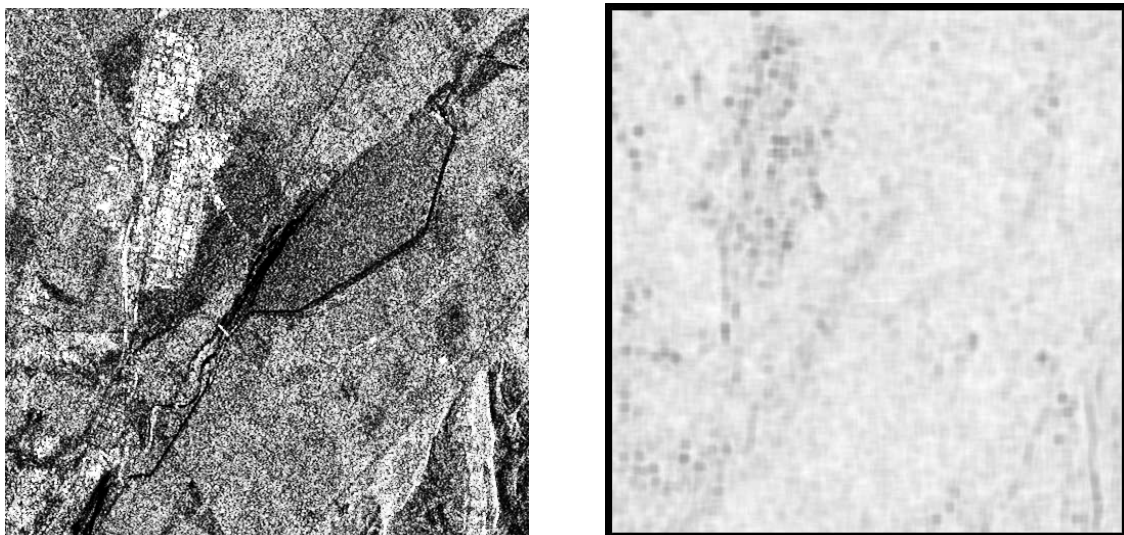


Fig. 10 Fractal transform: urban area segmentation in SAR scene

5. Conclusions

The developments in fractals theory opened new directions for research in scene and image synthesis and analysis. The close-fractal behaviours of the natural landforms makes fractal geometry to find one of the best fitted applications in geo-information processing.

One of the last trends in model based image analysis is to use geometrical models. The fractal geometry gives tools for the synthesis of models to be used in remotely sensed images interpretation. The scene and image synthesis are also extensively used in geomorphology. Terrain roughness, vegetation cover, can be accurately modelled. The simulation of the radiometric behaviours will enhance the understanding of image formation process both for optical and SAR sensors. Image analysis will also benefit from the advances in the field of fractal transform, and application of multiresolution and wavelet theory.

6 Bibliography

- *N.M. Allinson, M. Lawson, **Accurate Texture Characterisation Using Fractal Techniques**, IEE Colloquium on: "The Application of Fractal Techniques in Image Processing", Dec. 1990.
- *Stefano Baldo, **Introduction a la topologie des ensembles fractals**, Ecole polytechnique de Montreal
- *Jacques Belair, Serge Dubuc (Editors), **Fractal Geometry and Analysis**, NATO ASI Series, Vol. 346, Kluwer Academic Publishers, 1991.
- *Keith Clarke, **Scale-Based Simulation of Topographic Relief**, The American Cartographer, Vol.15, No.5, April 1988
- *Keith Clarke, Diane Schweitzer, **Measuring the Fractal Dimension of Natural Surfaces Using a Robust Fractal Estimator**, Cartography and Geographic Information Systems, Vol.18, No.1, 1991
- *M. Datcu, B. Dugnol, A. Lana, **Relief erosion - animation**, Dept. of Mathematics, University of Oviedo, 1991.
- *S. Dellepiane, D.D. Giusto, S.B. Serpico, G. Vernazza, **SAR image recognition by integration of intensity and textural information**, Int. J. Remote sensing, 1991, Vol.12, No.9.
- *Nigel Dodd, **Multispectral texture synthesis using fractal concepts**, IEEE Tr. PAMI, Vol. 9, No. 5, 1987.
- *J.L. Encarnacao, H.-O. Peitgen, G. Saks, G. Englert, **Fractal Geometry and Computer Graphics**, Springer-Verlag, 1992
- *Kenneth Falconer, **Fractal Geometry, Mathematical Foundations & Applications**, Wiley & Sons, 1992
- *Jens Feder, **Fractals**, Plenum, 1988
- *G. C. Freeland, T. S. Durrani, **On the use of the wavelet transform in fractal image modelling**, IEE Colloquium on: "The Application of Fractal Techniques in Image Processing Dec. 1990.
- *A. Glassner, **Graphic Gems 1**, 1991.
- *M. Goodchild, **Fractals and the Accuracy of Geographical Measures**, Mathematical Geology, Vol.12, No.2, 1980.
- *M. Goodchild, **The fractional Brownian process as a terrain simulation model**, Modelling and Simulation conference, Pittsburgh, Pa. 1982.
- *B. Goel, I. Rosenthal, R.L. Thompson, **A Computer Graphic Based Model for Scattering from Objects of Arbitrary Shapes in the Optical Region**, Int. J. Remote Sensing, Feb. 1990.
- *P. Hanusse, P. Guillaud, **Dendritic Analysis of Pictures, Fractals and other Complex Structures**, in: J.L. Encarnacao, H.-O. Peitgen, G. Saks, G. Englert, **Fractal Geometry and Computer Graphics**, Springer-Verlag, 1992
- *M. Hata, **Topological aspects of self-similar sets and singular functions**, in: **Fractal Geometry and Analysis**, NATO ASI Series, Vol. 346, Kluwer Academic Publishers, 1991.
- *Jie Huang, Donald Turcotte, **Fractal image analysis: application to the topography of Oregon and synthetic images**, J. Opt. Soc. Am. A, Vol 7, No. 6, 1990.

- *Dwight L. Jaggard, Xiaoguang Sun, **Scattering from fractally corrugated surfaces**, J. Opt. Soc. Am. A, Vol 7, No. 6, 1990.
- *C. Jones, P.G. Earwicker, S. Addioson, S. Watson, **Multiresolution Decomposition of Fractal Images**, IEE Colloquium on: "The Application of Fractal Techniques in Image Processing Dec. 1990.
- *James M. Keller, Susan Chen, **Texture Description and Segmentation through Fractal Geometry**, CVGIP, 45,1989.
- *L.M. Linnett, S.J. Clarke, **The Use of Fractal Modelling in texture Analysis**, IEE Colloquium on: "The Application of Fractal Techniques in Image Processing", Dec. 1990
- *A. Lindenmayer, **Mathematical model for cellular interaction in development**, Journal of Theoretical Biology, No.18, 1968.
- *Stephane G. Mallat, **A Theory for Multiresolution Signal Decomposition: The wavelet Representation**, IEEE Tr. on PAMI, Vol.11, No.7, July 1989.
- *B. B. Mandelbrot, **The fractal geometry of nature**, W. H Freeman, New York, 1982.
- *Uwe Mussigmann, **Texture analysis using fractal dimension**, in: J.L.Encarnacao, H.-O. Peitgen, G.Saks, G. Englert, **Fractal Geometry and Computer Graphics**, Springer-Verlag, 1992
- *H.-O. Peitgen, J.M.Henriques, L.F. Penedo (Editors), **Fractals in the Fundamental and Applied Sciences**, North-Holland, 1991.
- *H.-O. Peitgen, H. Jurgens, D. Saupe, **Chaos & fractals: new frontiers of science**, Springer-Verlag, 1992.
- *S. Peleg, **Multiple resolution texture analysis and classification**, IEEE Tr. PAMI, -6, No. 4, 1985.
- *Alex P. Pentland, **Fractal-Based Description of Natural Scenes**, IEEE Tr. PAMI, Vol.6, No.6, Nov. 1984.
- *L.Polidori, J.Chorowicz, **Modelling Terrestrial Relief with Brownian Motion: Application to Digital Elevation Data Evaluation and Resampling**, EARSeL Symposium, Graz, 1990.
- *L.Polidori, J.Chorowicz, R.Guillande, **Description of Terrain as a Fractal Surface, and Application to Digital Elevation Model Quality Assessment**, Photogrammetric Engineering & Remote Sensing, Vol.57, No.10, Oct.1991.
- *F. P. Preparata, R.T. Yeh, **Introduction to Discrete Structures**, Addison-Wesley, 1973.
- *P. Prusienkiewicz, J.Hanan, **Lindenmayer Systems, Fractals, and Plants**, Springer-Verlag, 1989
- *Anne Schistad, Anil K. Jain, **Texture analysis in the presence of speckle noise**, IGRASS'92
- *K. Seidel, M. Datcu, **Model based image analysis for remotely sensed images**, to be published.
- *A. R. Smith, **Plants, fractals, and formal languages**, Computer Graphics, 18(3), 1984.
- *Harry F. Smith, **A garden of fractals**, in: H.-O. Peitgen, J.M.Henriques, L.F. Penedo (Editors), **Fractals in the Fundamental and Applied Sciences**, North-Holland, 1991.
- *J. M. Soto-Crespo, M. Nieto-Vesparianas, **Electromagnetic scattering from very rough random surfaces and deep reflection gratings**, J. Opt. Soc. Am. A, Vol 5, No. 6, 1990.
- *Donald L. Turcotte, **Fractals and chaos in geology and geophysics**, Cambridge University Press, 1992.
- *R. F. Voss, **Random fractals forgeries**, in: Fundamental algorithms in computer graphics (Ed.: R.A. Earnshaw), Springer-Verlag, 1985.
- *R.F. Voss, **Random fractals: Characterisation and measurements**, in: Scaling Phenomena in Disordered Systems, (Ed.: P. Pynn, A. Skjeltrep) Plenum, 1986.
- *R. F. Voss, **Fractals in Nature: from characterisation to simulation**, in The Science of Fractals Images (Ed.: H. Peitgen, D. Saupe) Springer-Verlag, 1988.
- *Gregory W. Wornell, **A Karhunen-Loeve-like Expansion of 1/f Processes via Wavelets**, IEEE Tr. on Inf. Theory, Vol.36, No.4, July 1990.
- *Naokazu Yokoya, Kazuhiko Yamamoto, Noboru Funakubo, **Fractal-Based Analysis and Interpolation of 3D Natural Surface Shapes and Their Application to Terrain Modelling**, CVGIP, 46, 1989.